A study of the stellar populations in the Kepler field

Mark O'Reilly

Lund Observatory
Lund University

2017-EXA118

Degree project of 15 higher education credits
May 2017

Supervisor: Sofia Feltzing

Lund Observatory
Box 43
SE-221 00 Lund
Sweden

Abstract

Studying the formation and evolution of galaxies is a fundamental problem in astronomy that warrants repeated investigation by astronomers. How do spiral galaxies like our own come to have its distinct spiral arms? How do stars and their properties change over time and will they continue to evolve in the same manner? To try and attempt to answer such questions we need to look to our own Galaxy the Milky Way. Models have become an integral part of developing our understanding of the Galaxy but for these models to produce reliable data from which conclusions can be made upon, they must be shown to produce accurate and reasonable results. In this study a population synthesis code that produces synthetic stellar photometric data is compared to two surveys, 2MASS and Pan-STARRS, to analyse properties such as the total number counts and colour distributions. The parameters in the model were then changed in order to investigate how these effected the model's output. It was found from the different catalogues that the number counts from the model returned fewer stars, the amount of which varied with Galactic latitude with better agreement for the 2MASS survey. The colour of the model was then compared and found that for 2MASS the fit was much better than that of Pan-STARRS and that at higher Galactic latitudes the fit was slightly better. Investigating the input parameters to the model found that no change in the age metallicity relation and star formation rate in the thin disk gave any noticeable difference to either number counts or colour distribution, but for the case where no extinction was selected there were small changes in number counts for Pan-STARRS and expected changes in the colour distribution for both surveys. The initial mass function was also changed but it was found that the default Chabrier lognormal function was the best in simulating observed number counts.

Populärvetenskaplig beskrivning

Det är uppskattat att det finns fler stjärnor i universum än vad det finns sandkorn på jordens stränder och öknar tillsammans. Precis som stränder och öknar formar vår värld formar stjärnor vår galax och det bortom denna, och precis som att ett sandkorn är för lite för att berätta något viktigt om en strand, ger en stjärna inte mycket information till astronomer. Men många stjärnor i ett till varandra närliggande område kan hjälpa till att måla en bild av det stjärnområdet. I denna artikel testas en modell för stjärnutveckling mot verklig data, och vidareutforskas för att kunna göra valida pståenden om de stjärnor vi studerat. Modellering har blivit centralt inom astronomin för att frstå galaxen och vår plats i den. Det är därför viktigt att modellerna testas så de korrekt återger data, för att sedan kunna använda modellerna för att göra antaganden som förhoppningsvis kan leda till nya upptäckter. Detta projekt uppmärksammar och ifrågasätter användbarheten och tillämpningen av modeller över olika ämnen, samt belyser några några av de förhållanden som formar stjärnutveckling, t.ex. en stjärnas inledande massa eller de olika beståndsdelarna i Vintergatan. Rymden kommer att fortsätta att intressera oss, men om vi vill fördjupa vår förståelse kring de underliggande lagarna och principerna i rymden behöver vi mer exakta och förfinade modeller.

Stjärnor har olika temperaturer som påverkar vilken färg ljuset de avger har, denna färg kan undersökas för att ge oss information om enstaka och grupper av stjärnor. De kan avslöja en stjärnas ålder, var den befinner sig i stjärnutvecklingen samt deras kemiska beståndsdelar. Att använda färg för att kartlägga universums stränder och öknar är ett nyckelområde inom astronomin, som leder till nya upptäckter och fortsätter att ge oss en detaljerad karta över galaxen och vår plats i den.

Contents

Chapter 1

Introduction

1.1 Modelling the Milky Way

The Milky Way galaxy is of special importance as it is the galaxy that we can study in the greatest detail, from regions of HII gas, which help astronomers tell where there are clouds of atomic hydrogen and new star formation to something as simple as distance through parallax measurements of nearby stars. It is a great source of information giving astronomers insight into its formation and evolution. Our position within a spiral arm known as the Orion Spur gives a unique view of our Galaxy as it means we sit in the plane of what's known as the disk, allowing observations along this plane towards the Galactic centre and towards the outer edges. Stars close to our position offer the most detailed picture of local stellar groups in spiral galaxies like our own. Stars have been documented with regards to their brightness from Earth and relative position from up to 2 000 years ago by the Greek astronomer Hipparchus who categorised stars according to their brightness, with brighter stars having a lower magnitude of 1 and fainter ones 6. This system formed the basis of the magnitude system used in modern astronomy today.

The evolution of galaxies is an incredibly complex process for which there are many fields of research, each trying to unlock answers to some of the key questions with the help of models. How did galaxies first form and is their present day form shaped from the merging of smaller galaxies? According to ΛCDM, a parameterisation model of the Big Bang that best describes the large-scale structure of the universe, a galaxy like our own has suffered bombardments of merging blocks over its life time (Bensby & Feltzing 2010). Another area of research into galaxy evolution is that of the star formation rate and history within the Milky Way, which has been estimated to be around 1.9 $M_{\odot}yr^{-1}$ (Chomiuk & Povich 2011). These are just two examples of the wide-ranging research areas that surround galaxy evolution.

Light from a star carries a lot of information, which astronomers use to determine certain properties about that star. Stars have different chemical compositions and ages which will affect the colour of light emitted, and the wavelength of light can help tell us the temperature from using blackbody radiation and Wien's displacement law which states

that the peak of the radiation curve is dependant upon only the surface temperature. So it is clear that the light from a star is a useful tool for analysis. To help represent and display relations between a star's colour and its other parameters colour magnitude diagrams (CMD) are constructed. Whereas Hertzsprung–Russell (HR) diagrams show the relationship between a star's temperature and its luminosity or absolute magnitude, a CMD describes the relation between colour and apparent magnitude. Thus to plot HR diagrams the distance to the stars needs to be known so the absolute magnitude can be calculated, which can be done through the distance modulus equation

$$m - M = 5\log_{10}(d) - 5 \tag{1.1}$$

where m and M are the apparent and absolute magnitudes respectively and d the distance to the stars in parsecs.
The colour of a star, obtained from the measurement of a star in a specific filter defined around a specific wavelengths, is far easier to measure and doing so is much more time efficient than taking the whole spectrum of a star, and CMDs can be used to plot stars whose distance is not known. These diagrams show details such as the different evolutionary stages and within these 'branches' the shape and colour can be used to infer certain properties about the stellar population, such as its metallicity. The metallicity of a star is defined typically as the ratio of Iron to Hydrogen in the star and is a logarithmically normalised scale against the Sun. It can be applied for other elements (x in the equation below refers to any element with a higher atomic number than helium) as well, but the iron ratio is most commonly used

$$[x/H] \equiv \log_{10}\left(\frac{n(x)}{n(H)}\right)_{\star} - \log_{10}\left(\frac{n(x)}{n(H)}\right)_{\odot} \tag{1.2}$$

Astronomers would like to try and discover the history and predict the fate of our Galaxy and others alike. To understand the evolution of our Galaxy, we first need to know what it has evolved into. It is therefore necessary to understand the different Galactic components that the Milky Way is comprised of and how these shape its structure. The Milky Way is a barred spiral galaxy that contains a central bulge from which a bar spreads out to form the base of the spiral arms. Its main Galactic features are the thin and thick disks, halo and bulge. In the centre of the Galaxy lies a supermassive black hole around which the Galaxy rotates taking an estimated 225 million years to complete one full rotation.

1.2 Milky Way and its components

Bulge

The Galactic bulge as defined in Vanhollebeke et al. (2009) refers to Galactic components in the direction of $|l| \leq 10°$, l being the Galactic longitude[1]. It hosts a variety of stars such

[1]Galactic longitude is the angle from the Galactic centre along the plane and latitude is the angle above the Galactic plane

as old, metal poor RR Lyrae stars as its inner most inhabitants. It has been postulated that these metal poor stars in the inner bulge may be the oldest population in the Galaxy (Minniti & Zoccali (2008)). Throughout the bulge, old populations comprise approximately 90 % of the stars.

Thick disk

The older of the two disks, the thick disk has a scale length of 2 500 pc and scale height[2] of around 1 kpc, about four times larger than the scale height of the thin disk. One possible hypothesis of the formation is believed to have arisen from the heating of the early stellar disk by accretion events (Freeman & Bland-Hawthorn (2002)). It is populated with mostly older and more metal poor stars. The ages of the stars vary but are older than those of the thin disk. Star formation ceased some time ago, roughly after 5 Gyr (Snaith et al. 2015). The thick disk presents a modern day snapshot of the early disk making it an invaluable source for the study of early processes of the Galaxy.

Thin disk

The thin disk is a place of active star formation and is host to mostly younger more metal rich stars. It is estimated to have a scale length of 3000 pc and scale height of 250 pc (Bland-Hawthorn & Gerhard (2016)). These younger stars were born in molecular clouds more enriched with metals from the supernovae and solar winds of earlier stars hence the typically higher metallicity content. The age spread of the stars in the thin disk results in a variety of stars in different stages of their stellar evolution. Once stars run out of hydrogen to burn, their cores contract under the gravitational pressure inducing higher temperatures and He shell burning begins. The temperature gradient of the star steepens inducing convection whose envelope then expands and so the star becomes a red giant. These can be found in all components and form a distinct feature on a HR diagram, discussed later.

In the thin disk component there is a lot of interstellar gas and dust which scatters light as it passes through. This causes stars to appear slightly fainter than they really are and also changes the apparent colour since the scattering is wavelength dependant; shorter wavelength light is scattered by the dust grains more than longer wavelengths. The extinction coefficient describes the change of apparent magnitude m compared to that without absorption m_0.

Halo

Stretching roughly 40 kpc across some of the earliest stars to form in the Galaxy now reside here. The stars in the halo are extremely metal poor as they were some of the first stars to

[2]Scale height is the distance at which the number density of stars decreases by a factor of 1/e, the scale length is the same but in the horizontal plane of the Galaxy

form and can be distinguished by their random, high velocity orbits. Star forming activity ended some time ago, and the majority of the space here is empty. Encompassing the halo is a dark matter halo, extending far beyond the reach of the halo but its properties are mostly unknown due to the elusive nature of dark matter.

1.3 Models and their place in science

In this work I have investigated a population synthesis model that simulates stars and their photometric data, but first we should ask the question of why models are so important and how they can be used to investigate stellar relations and properties. As in many other areas of science models are created so that scientists can reproduce observed data and investigate physical phenomena allowing a deeper understanding of how the world around us works. Trilegal (Girardi et al. 2005), the population synthesis code investigated in this paper, makes use of theoretical and empirical data to simulate stellar evolution as described in Chapter 3. Once a model finds supporting evidence and is accepted one can then use that model to confidently make reliable predictions about the phenomena it represents. The model is then a time efficient way to investigate the evolution and formation of the Galaxy by creating a replica Milky Way and then pushing fast forward to the present day in an instant.

For the different Galactic components there are different values for properties such as scale lengths and heights, distance to the Galactic centre and absorption coefficients. Accurate models can help ascertain the true value of these parameters as changing these parameters will change the output of the models. When the output consistently matches that of observed data you can then make claims about the parameters and their influence on the properties of the Milky Way. But for all this data the model produces there has to be detailed catalogues and surveys of real, empirical data of stellar populations so that comparisons can be made. Humans have come a long way from merely looking up at the sky with the naked eye. Advancements in optics have allowed the construction of better telescopes allowing us to see in greater detail what was once hidden in plain sight. Infrared telescopes have allowed astronomers to gain a more detailed view by seeing through the interstellar gas and dust that resides throughout the interstellar medium and microwave telescopes have allowed the mapping of the earliest Universe roughly 300 000 years after the Big Bang via the WMAP observatory (Komatsu et al. 2011). The further development of optical abilities will continually expand our knowledge and mapping of the Milky Way, with current missions such as Gaia aiming to chart a three dimensional map of the Galaxy and its structures. Future telescopes such as the Large Synoptic Survey Telescope, due to launch in January 2022, will undertake a ten year survey the result of which "will be astronomical catalogues thousands of times larger than have ever previously been compiled containing the data necessary to begin searching for answers" (Ivezic et al. 2009).

1.4 Implementation of investigation

Next, the two surveys used in this paper and their background are described, followed by a detailed description of Trilegal itself. After comparing initial results of the surveys and the model, certain parameters are changed in the model to note what happens and an attempt is made to explain the changes seen. Firstly the number counts are compared through diagrams and the ratio of the number counts per magnitude bin is taken. Then the colour distributions are compared through CMDs and details of these diagrams are discussed.

Chapter 2

Data

The two sets of data used to test the workings of Trilegal are the Panoramic Survey Telescope & Rapid Response System (Pan-STARRS) survey (Chambers et al. 2016) and the Two Micron All Sky Survey (2MASS) (Skrutskie et al. 2006). These tell us the apparent magnitude of stars in the different passbands defined by their photometric systems. In both data sets the distances to the observed stars are not known, and every measurement carries an associated uncertainty. Both data sets probe similar magnitudes, with Pan-STARRS covering magnitudes in a range from $13 < m_g < 23$ and 2MASS $11 < m_J < 17$.

The stars analysed in this project are located within the Kepler field, a portion of the sky that has a field of view (FoV) equal to 105 $\deg^2$ located next to the constellation Cygnus. The total field is made up of 21 CCD modules, which cover 5 $\deg^2$ each. Initially picked as a suitable location for the search for exoplanets, it was found to contain large numbers of stars of which good quality data could be recorded. Each search catalogue is centred around specified coordinates and uses the cone search method. This means that the area covered in the search catalogue takes the shape of a cone from Earth's position. The end of this cone is a circle and corresponds to a radius of 15 arcminutes, meaning the catalogues cover a FoV equal to 0.2 $\deg^2$.

The Kepler field, originally chosen as a suitable location for the search of expolanets whereby the stars are nearly continuously viewed at one FoV carefully selected to provide an appropriate density of target stars (Haas et al. 2010), makes it an ideal location for the this paper to conduct its comparison. As seen in Fig. 2.1 the Kepler field is located very close to the Galactic plane sweeping from the bottom left of the picture and so stars from catalogues here will consist of a mixture of disk and halo stars. The table below details the centre of three search catalogues. Henceforth the position of each catalogue is defined in conjunction with top, middle and bottom by the Galactic latitude with the highest value representing the top of the Kepler field.

Table 2.1: Centre of search catalogues

	Celestial Coordinates	Galactic coordinates [°]
Top	19h14m 51°30'	l = 82.3° b =17.6°
Middle	19h40m 45°	l = 78° b = 11°
Bottom	19h54m 39°46'	l = 74.8° b = 6.2°

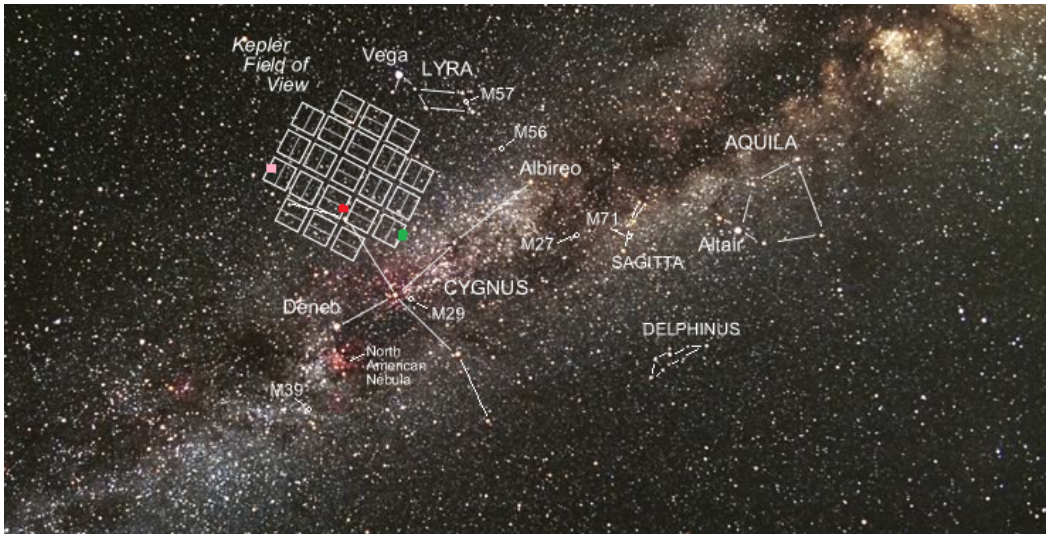

Figure 2.1: The Kepler field divided into each of its 21 CCD modules. Search catalogues at top, middle and bottom coloured by the pink, red and green circles respectively. Figure obtained from Kepler.nasa.gov.

2.1 2MASS

Starting in June 1997 and finishing in 2011, the Two Micron all Sky Survey is the collective result from two telescopes surveying the sky in the near infrared. The observations were carried out from two 1.3 m equatorial Cassegrain telescopes, one in either hemisphere located in Mt Hopkins, Arizona, and Cerro Tololo, Chile and together they cover 99.998% of the sky (Skrutskie et al. (2006)). The three photometric bands used are the J (centred at 1.25 μm), H (1.65 μm), and Ks (2.16 μm) where Ks stands for 'K-short', meaning that the passband excludes wavelengths longward of 2.31 μm (Skrutskie 2006). Fig, 2.2 shows the passband curves of the three filters. It is worth noting that the 2MASS data was one of a few data sets that Trilegal was modelled and tested against whilst under construction. An immediate advantage of 2MASS is that its passbands are in the near infrared spectrum. This means that whilst observing the Milky Way and beyond, extinction becomes much less problematic compared to visible wavelengths. The on-line catalogue and canonical paper for 2MASS can be found at `http://irsa.ipac.caltech.edu/Missions/2mass.html`.

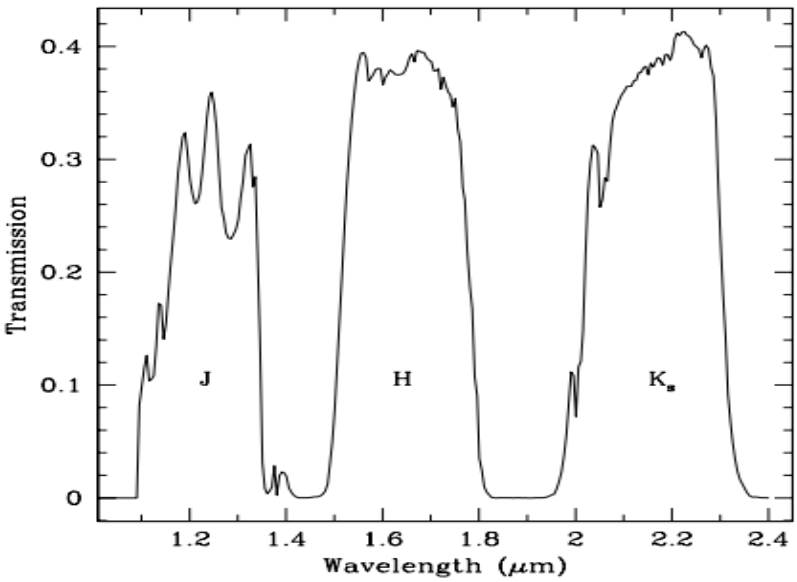

Figure 2.2: Passband curves for 2MASS. Figure obtained from Skrutskie et al. 2006

2.2 Pan-STARRS

The Pan-STARRS survey (Chambers et al. 2016) was carried out on the summit of Halekala in Hawaii, surveying the sky over a four-year period, from 2010 till 2014, using the PS-1 telescope with a 1.8 m diameter primary mirror. One of the primary goals of this survey was to survey the solar system including potentially hazardous, near Earth asteroids and to obtain precision photometric data of stars in the Milky Way and local group (Chambers et al. (2016)). The photometric system uses 5 passbands starting in the visible region. These passbands are g_{P1} (centred at 4770 Å), r_{P1} (6231 Å), i_{P1} (7625 Å), z_{P1} (8679 Å) and y_{P1} (10 000 Å). The $_{P1}$ notation is to distinguish PS1 from other photometric systems. The filter curves are seen in Fig. 2.3, obtained from Tonry et al. (2012). The search catalogue for Pan-STARRS can be found at `http://archive.stsci.edu/panstarrs/search.php`.

Both data sets use the cone method and as such, the further from Earth one travels the greater the cross sectional area of the cone becomes. As a result, the volume covered by the search close to Earth will be far less than an equidistant distance further out in space. This leads to a selection bias in the catalogues meaning we'll observe more stars further away than close to the Earth.

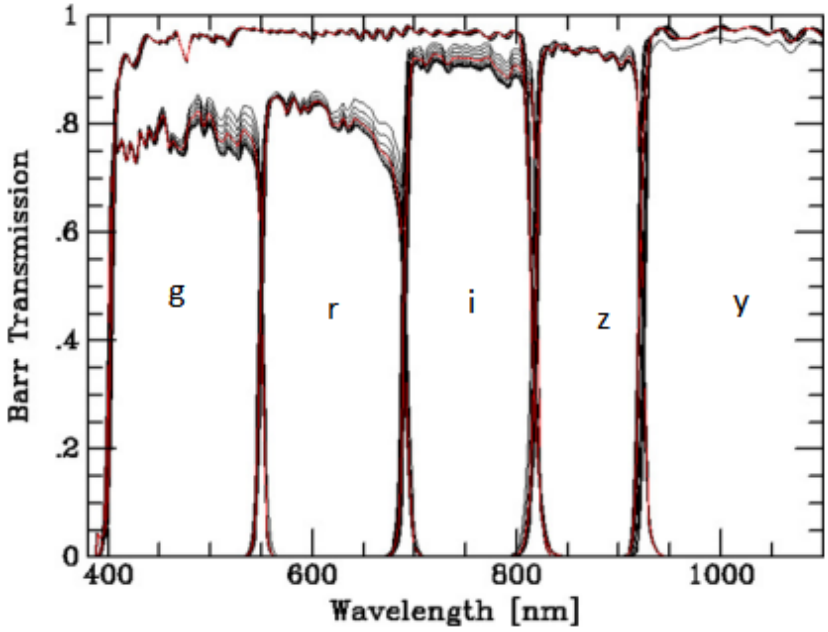

Figure 2.3: Passband curves for Panstarrs. Barr transmission corresponds to the filter transmission of Pan-STARRS which is manufactured by Barr Precision Optics

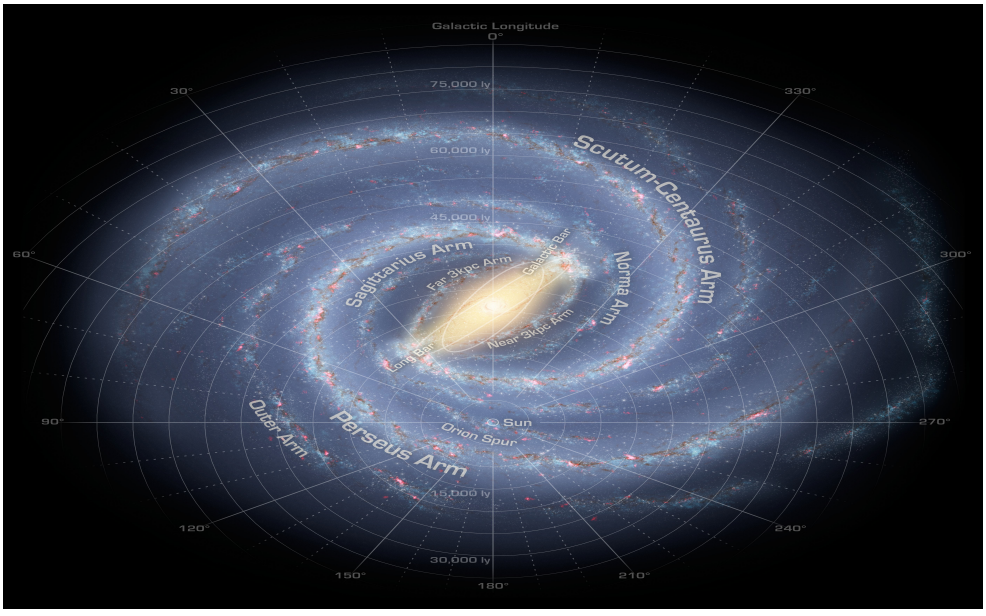

Figure 2.4: Location of the Sun within the Milky Way. Looking at the Galactic longitude one can see the direction of the Kepler field, with Galactic longitudes around $l = 70°$, to the left and away from the Galactic centre. Figure obtained from nasa.gov.

Chapter 3

Trilegal

3.1 TRIdimensional modeL of thE GALaxy

Trilegal is a population synthesis code that simulates stellar evolution to output stellar photometry for the different parts of the Milky Way. The code is written in the C language and it can be found on-line at its homepage `http://stev.oapd.inaf.it/cgi-bin/trilegal`. The primary goal of Trilegal as stated in Girardi et al. (2005) is to simulate expected star counts in different passband systems. Its second goal is to be able to reproduce photometric data from very shallow surveys through to much deeper surveys.

A run through in Trilegal represents a Monte Carlo simulation whereby star counts are generated by the fundamental equation of stellar statistics which describes the number of stars per bin of distance modulus. Here r is the line of sight distance, $\rho(r)$ the stellar density at position r and $\phi(M_{\lambda,0},r)$ is the intrinsic distribution of stellar absolute magnitudes.

$$N(m_\lambda.l,n) = dm_\lambda \int_0^\infty drr^2\rho(r)\phi(M_\lambda,r)d\Omega \tag{3.1}$$

Each star then utilises the input star formation rate (SFR), age metallicity relations (AMR) and the initial mass function (IMF) to single out the stellar age, metallicity and mass. Trilegal is comprised of four main elements: libraries of theoretical evolutionary tracks; a synthetic spectra library; different filter systems; and a description of the Galactic components. The output of a Trilegal run results in a large data file consisting of different columns giving information for each star such as age, metallicity, distance modulus and surface gravity. The end columns output the apparent magnitudes in the relevant passbands. Its worth noting that the output is a 'perfect photometric catalogue' meaning there are no associated errors for the apparent magnitudes.

The input to Trilegal is found on-line at the aforementioned link. It consists of different sections within which different parameters can be changed. The first four sections describe the pointing parameters in both Galactic and equatorial coordinates along with a size in deg^2 of the search area covered, the photometric system that you want to replicate with a limiting magnitude in one of the filters (to prevent the generation of too many faint stars),

the IMF to be used and the extinction, described later. The major components of the Milky Way follow: the thin and thick disks have scale heights and lengths, both of which can be changed; the Halo; finally and bulge components. Apart from the thick disk all four have two options for the SFR and AMR.

The thin disk takes the form of a squared hyperbolic secant function whereby the scale height is assumed to increase with age, t, and variable parameters α and z_0 via the equation

$$h_d(t) = z_0(1 + t/t_0)^\alpha \tag{3.2}$$

Thus closer to the Galactic plane stars are formed and then disperse vertically. The thick disk has no such age relation but its scale height is also described by a squared hyperbolic secant function. The bulge and halo default parameters are described in Girardi (2005). Essential to the simulation of photometric data are the IMF, isochrones and the star formation rate.

Isochrones are theoretical constructs that map stars of varying mass at a certain point in time. A group of stars that formed at the same time [1], which is the case for clusters of stars, then evolve for a certain period of time and move position in the HR diagram. At a certain time, one then checks to see where the stars have evolved to, and a line can be drawn to trace through the positions of the stars. This line is known as a stellar isochrone. Having isochrones covering a wide range of ages gives one the ability to model stars of differing ages which can then be plotted in a CMD. Isochrones do not however tell us how many stars can be found where along the isochrone. For this, synthetic stellar populations are created using the IMF and at a given time the parameters describing these stars are taken from extensive libraries and plotted in a CMD. For a CMD to be plotted one needs to take the output of the model - such as effective temperature and surface luminosity- and covert them into observable quantities. This is done through bolometric corrections and effective temperature correlations but this is beyond the scope of this paper. For a detailed explanation and derivation into these two methods one should refer to Girardi et al. (2002). It is worthy to note that isochrone uncertainties for CMD fitting can lead to a slight source of error, for example when investigating the age metallicity relation (AMR) using isochrone fitting one can have bigger age uncertainties allowing younger ages for stars (de Boer et al. 2012).

The initial mass function is one of the most important astrophysical distribution functions and is essential to any modelling of stellar populations. It describes the amount of stars formed per unit mass during a single star forming event. Such an important parameter has warranted a lot of research and investigation into describing the IMF. The first key contribution came from Salpeter in 1955 whereby he described the IMF as a power law with a slope equal to 2.3. This translates to fewer high mass stars and greater lower mass stars. The stars initial mass is of great importance as it determines where along the zero age main sequence it falls which will heavily effect its subsequent evolution, with stars of greater mass burning through their hydrogen supplies and turning off the main sequence earlier than lower mass stars. The IMF in Trilegal is normalised so that it is for a total

[1] The word isochrone originates from the Greek words 'isos' and 'khronos', meaning equal and time.

mass equal to 1 solar mass i.e. $\int_0^\infty m\phi_m dm = 1M_\odot$.

The default IMF used in Trilegal is described by a Chabrier log-normal function described by

$$\phi_m \propto m \ \exp\left[- \frac{(\log\ m - \log\ m_0)^2}{2\sigma^2} \right] \tag{3.3}$$

where $m_0 = 0.1$ M$\odot$ and the dispersion $\sigma = 0.627$.

Along with the IMF, two other important astrophysical functions are the star formation rate (SFR) and age metallicity relation (AMR). The SFR is, as its name suggests, the rate of formation of stars throughout as a function of time given in $M_\odot$/yr. There is some debate as to whether the SFR is irregular or has been a constant rate, but in this paper the default SFR assumes that between 1 and 4 Gyr the SFR has been 1.5 times larger than at other ages and constant between 12 - 13 Gyr for the halo. The AMR is given by Z(t), where Z, the mass fraction of metals, can be converted to the standard logarithmic metal and iron contents through the approximate relations

$$[M/H] = \log(Z/Z_\odot) - \log(H/H_\odot)$$

and

$$[Fe/H] = \log(Z/Z_\odot) - [\alpha/Fe]$$

where $Z_\odot = 0.0019$. These approximations provide [M/H] and [Fe/H] values accurate to within ~ 0.03 dex.

There is also an extinction layer for the disks that assumes an exponentially decreasing density in the vertical direction specified by a scale height. There are two settings; one calibrated to infinity and one local calibration. The calibration at infinity means the same extinction irrespective of distance whereas the local calibration is given as 0.00015 mag/pc and thus changes with distance. The local calibration is the one used in this thesis.

Chapter 4

Investigation and results

4.1 Initial results

A good first comparison of Trilegal to the two data sets is the difference in the star counts. The rise in star counts is seen in Fig. 4.1 for both Pan-STARRS and 2MASS at latitudes of b = 17.6°, 11° and 6.2° within the Kepler field. The same graph but with a logarithmic scale can be found in Fig. A.1 in the appendix. The number counts of the first passband in each data catalogue are presented below

Table 4.1: Star counts for different search catalogues, with values on right representing the Trilegal data

	Pan-STARRS	2MASS
b = 17.6°	7 972 | 5 628	1 810 | 1 479
b = 11°	14 417 | 13 129	3 774 | 3 087
b = 6.2°	30 071 | 34 029	9 560 | 7 379

The ratio between the number counts per magnitude bin was taken to see if there was a constant offset between the Trilegal and observed data. The results for Pan-STARRS are shown in Table 4.3 and for 2MASS in Table 4.2. The counting of stars per magnitude bin can be considered a Poisson process since the process of observing the stars is independent of one another. When something follows a Poisson distribution the standard deviation will fluctuate around its mean by $\sqrt{N}$, N simply being the number of observed events. The deviation in the ratio is then $\sqrt{N}$ divided by the number count from Trilegal. This means that the error in readings is greater for bins at brighter magnitudes due to the lower number of stars counted in these magnitude bins compared to those at fainter magnitudes.

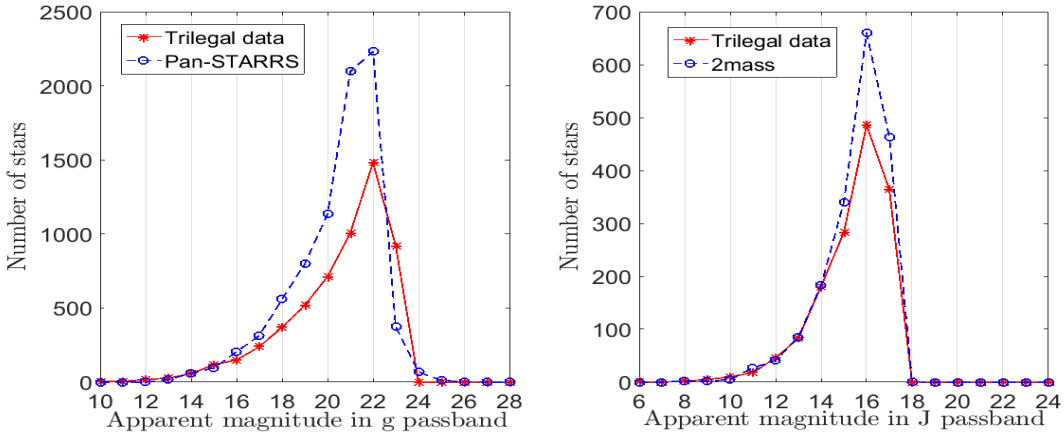

(a) b = 17.6°

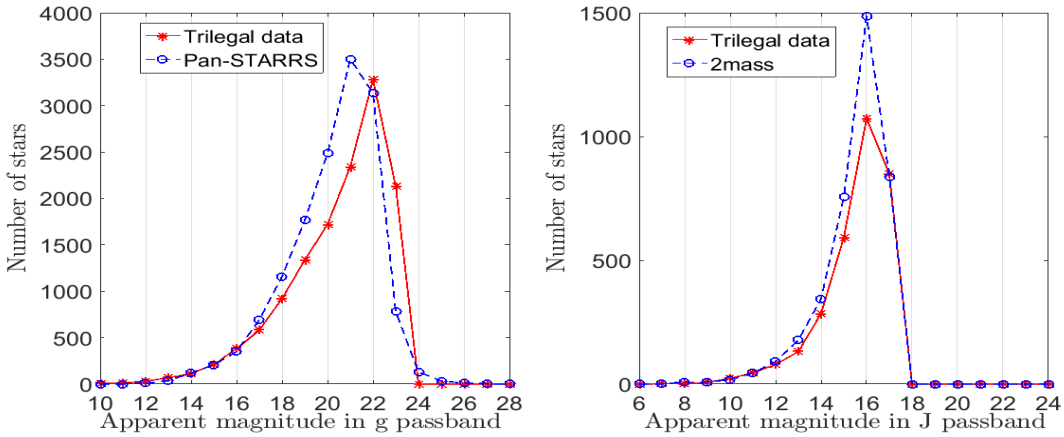

(b) b = 11°

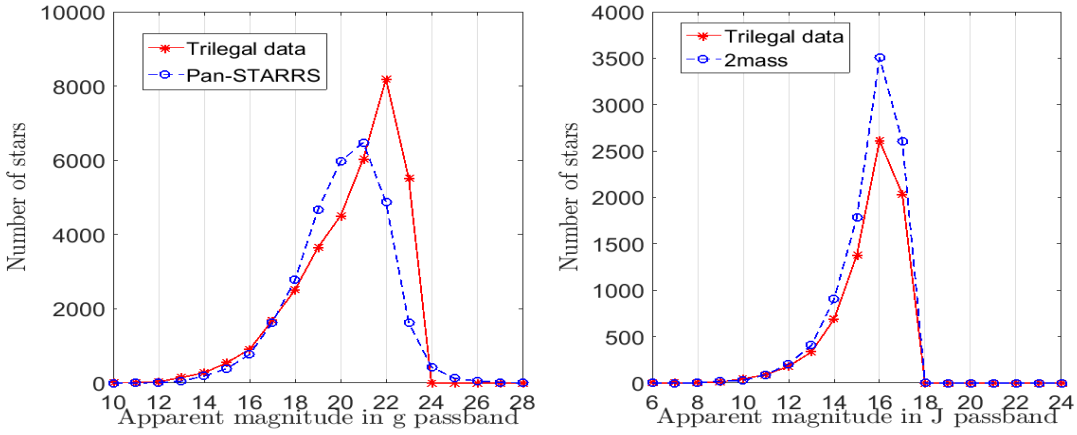

(c) b = 6.2°

Figure 4.1: Star counts for Pan-STARRS and 2MASS in the different search catalogues within the Kepler field.

Table 4.2: Ratio between number counts from Fig. 4.1 for 2MASS in descending order

magnitude	9	10	11	12	13	14	15	16	17
b = 17.6°	2.50	2.00	0.67	1.12	0.98	0.99	0.83	0.74	0.79
b = 11°	0.88	1.28	1.02	0.87	0.74	0.83	0.78	0.72	1.01
b = 6.2°	0.60	1.64	0.98	0.89	0.82	0.76	0.77	0.74	0.78

Table 4.3: Ratio between number counts from Fig. 4.1 for Pan-STARRS in descending order

magnitude	14	15	16	17	18	19	20	21	22
b = 17.6°	1.02	1.23	0.73	0.76	0.66	0.65	0.63	0.48	0.66
b = 11°	0.94	1.02	1.09	0.84	0.79	0.76	0.69	0.67	1.05
b = 6.2°	1.44	1.40	1.18	1.04	0.91	0.78	0.75	0.93	1.68

Another way of comparing the rise in number counts is through the Kolmogorov-Smirnov test (K-S test) whereby the cumulative distributions of the samples are compared. The K-S test returns three output arguments. First, the null hypothesis test result which compares the distribution of the two sets to determine if they are from the same continuous distribution. A value of h = 1 is returned if the null hypothesis is rejected, meaning the two distributions are not from the same continuous distribution. Second there is the probability p, being the probability of observing a test statistic as extreme as, or more extreme than, the observed value under the null hypothesis. Third and finally, the test statistic k which is the greatest difference between the CDFs of the distributions of the two data sets. Fig. 4.2 shows two of these tests and the output arguments can be seen in the table below

Table 4.4: K-S test results

(a) Pan-STARRS

	K-S h	Probability p	Test statistic k
b = 17.6°	1	4.2×10^{-63}	0.147
b = 11°	1	1.7×10^{-70}	0.152
b = 6.2°	1	0	0.167

(b) 2MASS

	K-S h	Probability p	Test statistic k
b = 17.6°	0	0.2151	0.031
b = 11°	1	1.23×10^{-6}	0.063
b = 6.2°	0	0.1183	0.016

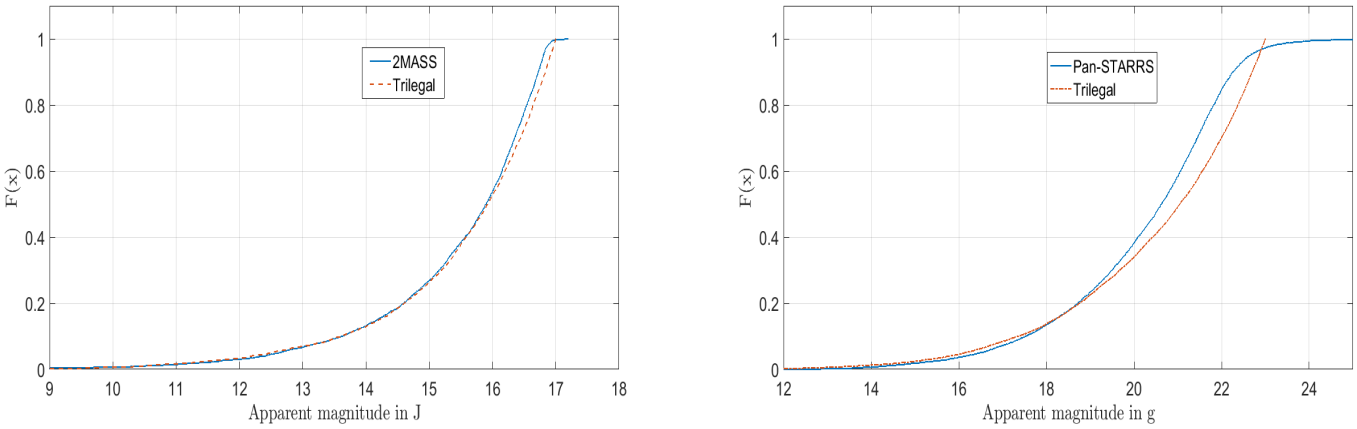

Figure 4.2: Cumulative distribution functions for 2MASS J passband and the Pan-STARRS g band, b = 11°. F(x) is the fraction of total stars observed.

The small k statistic from table 4.4 can be seen in the figure above since the two distributions are much closer and better fitted in the 2MASS figure, resulting in a smaller greatest distance of the CDFs. In both cases Trilegal starts simulating more stars at brighter magnitudes and then proceeds to simulate too few stars at fainter ones. This can be better seen in Fig. A.1, where for the model of Pan-STARRS Trilegal simulates too many stars at brighter magnitudes and then goes on to simulate too few, where the change in simulating too many to too few seems to come at fainter magnitudes at lower latitudes. 2MASS appears to do the same but not by as much, and typically fits the data curve far better at fainter magnitudes. A remark is made about Fig. 4.2, that perhaps a better representation of the CDFs would be made by having a magnitude limit at 17 and 23 for 2MASS and Pan-STARRS respectively. This is because of the completeness of the telescopes; a star at brighter magnitudes has a probability close to one of being detected but close to the magnitude limit the probability drops closer to zero. This limit is the completeness limit of the telescope, and so the same figures for b = 6.2° and b = 17.6° were produced but with a cut off in the data at the previously mentioned magnitude limits. These are seen in the appendix, Fig A.4.

4.2 CMDs

As mentioned before distances to stars in both Pan-STARRS and 2MASS are not known so an absolute magnitude vs. colour diagram is not possible. One of Trilegal's output columns is the distance modulus, and using equation (1.1) the absolute magnitude can be obtained allowing such a plot to be made. This shows the different evolutionary stages that the stars belong to.

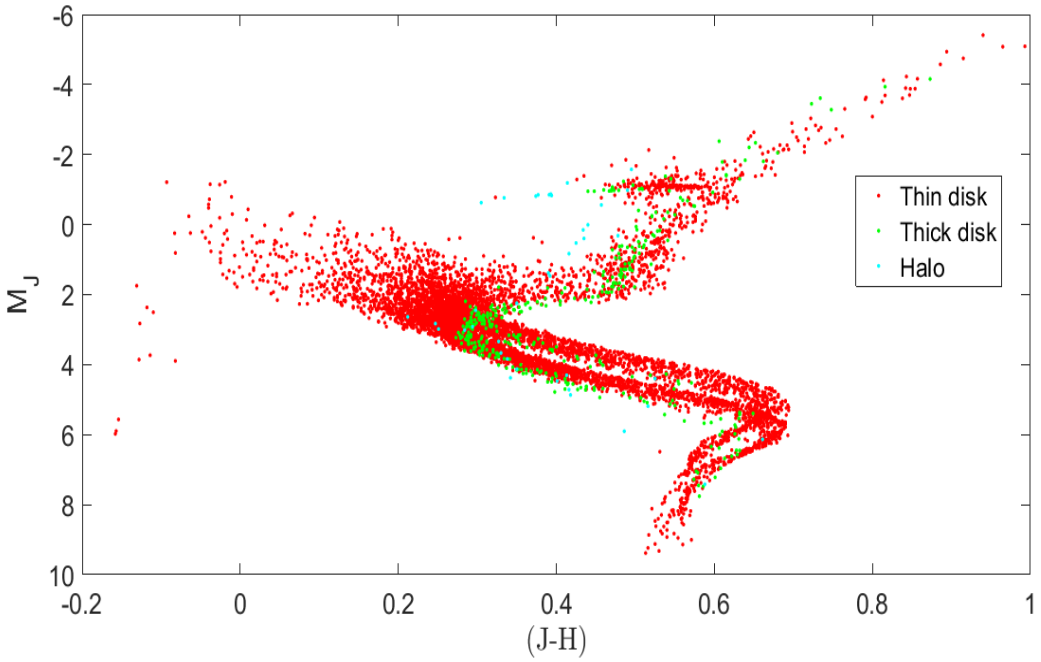

Figure 4.3: Absolute magnitude HR diagram for 2MASS, b = 6.2°. Noticeable from this figure is the lack of halo stars

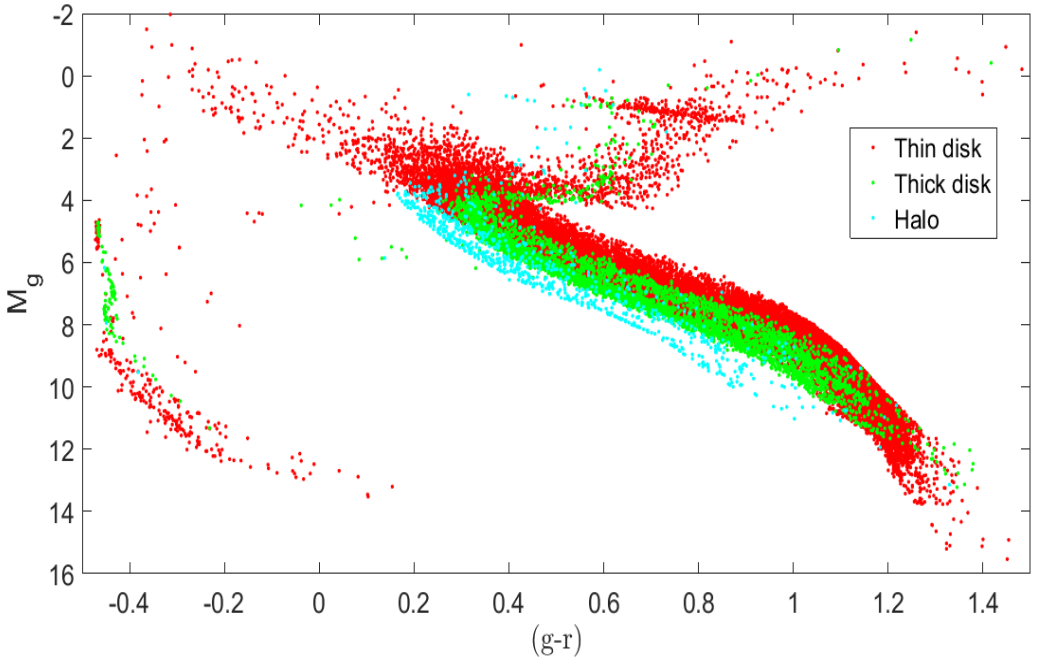

Figure 4.4: Absolute magnitude HR diagram for Pan-STARRS, b = 6.2°. The low metal halo stars reside along the bottom of the main sequence.

Why so few halo stars are present in the 2MASS HR diagram led to the investigation of the distribution of the distance modulus of the two models. The number counts per distance modulus were plotted and are shown in Fig. 4.5. One can see that 2MASS samples far fewer stars at greater distances and starts to decrease from 12, earlier than Pan-STARRS and as such probes far fewer halo stars than Pan-STARRS.

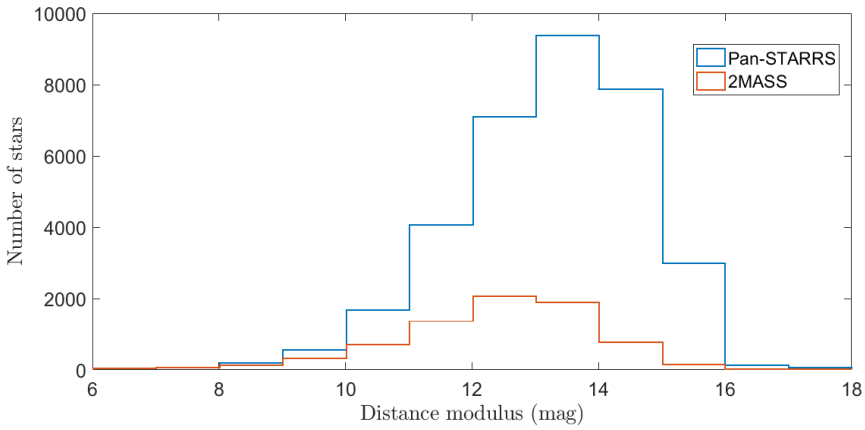

Figure 4.5: Distribution of star counts per distance modulus

Fig. 4.4 shows the main sequence section covering the majority of stars with a turn off close to (g-r) $\sim$ 0.2. Stars that have evolved off the main sequence then occupy the sub giant and giant branch. The sequence of stars slightly underneath the main sequence is formed of more metal poor stars, and the wide spread of the red giants may well be due to the aforementioned isochrone uncertainty whereby the stars occupying this region will have a wide spread in ages, but also due to the wide range in metallicities. The opacities of metals in the stellar envelope help determine the stars colour, with greater opacities meaning redder stars. In the bottom left white dwarfs are seen, which are considerably bluer than any of the other stars. This white dwarf section can be seen in Fig. 4.6 as the set of stars that occupy a colour of -0.5 $<$ (g-r) $<$ 0 in the bottom left part of the Pan-STARRS Trilegal CMD. The 2MASS HR diagram shows a similar pattern; a main sequence that looks to be comprised of two main sequences with the same turn off around (J-H) $\sim$ 0.25 followed by the sub giant and red giant branch. In both HR diagrams there is a slight horizontal clump of stars in the top part of the red giant branch which is the beginning of the horizontal branch. The same stars are then plotted into colour magnitude diagrams displayed in Fig. 4.6.

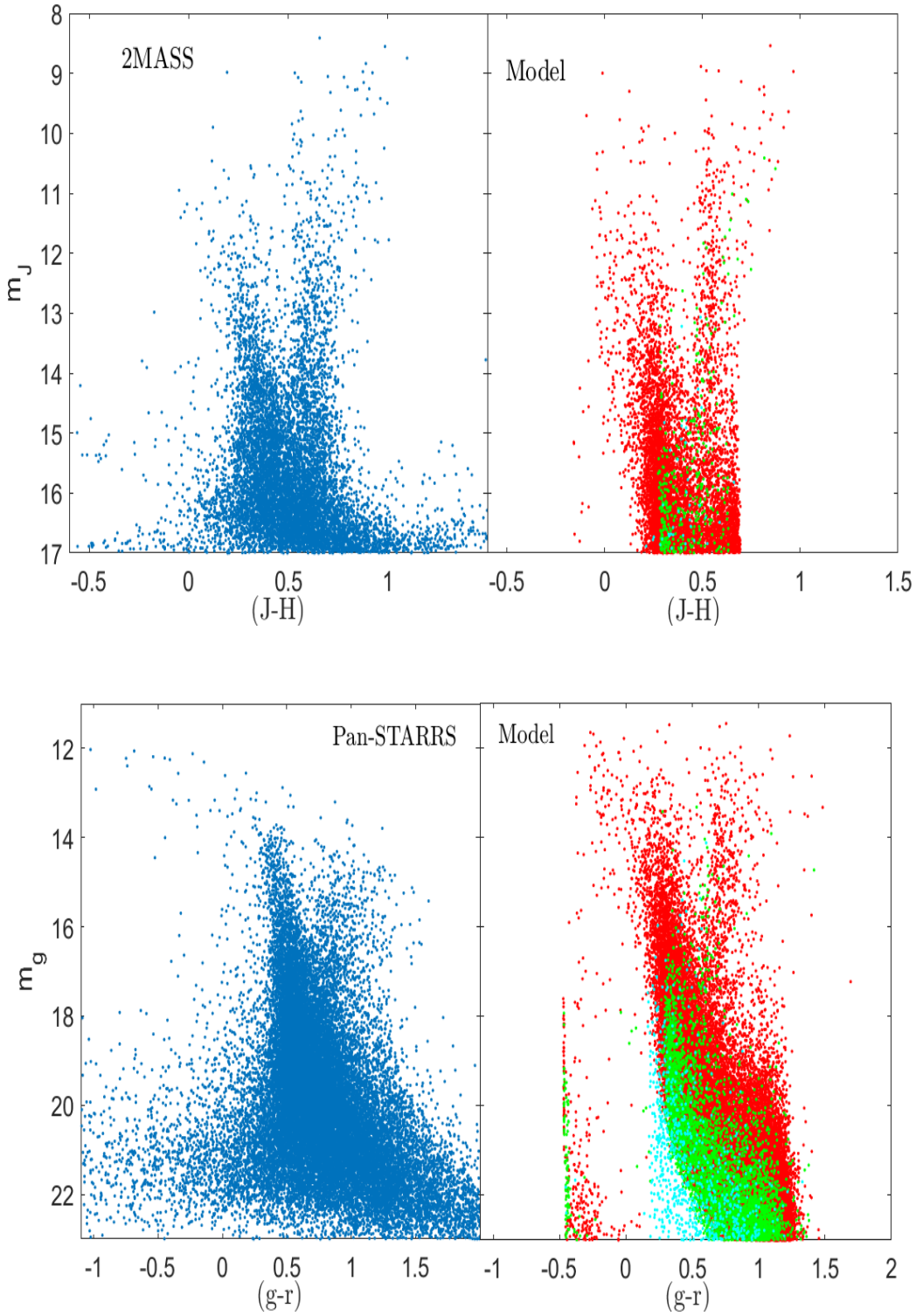

Figure 4.6: CMDs for 2MASS and Pan-STARRS and the corresponding Trilegal output. The colour schemes remain the same for the models.

We see from the 2MASS Fig. 4.6 a close similarity in the CMD's with a turn off around (J-H) $\sim$ 0.25. Both figures show two vertical structures with the one on the right probing brighter magnitudes in both cases. The right vertical structure covers a range of 0.4 $<$ (J-H) $<$ 0.7 which as seen from the 2MASS HR diagram consists of a combination of the stars on the bottom half of the main sequence along with the red giant and horizontal branch. The left vertical structure, from 0.2 $<$ (J-H) $<$ 0.4 covers mostly stars by the turn off and beginning of sub giant branch. The top of the vertical structures are more likely to be populated by mostly giants due to their highly luminous nature. The bottom will contain mostly main sequence stars. Looking at the Pan-STARRS CMD from Fig. 4.6, one can see an inconsistency as there is a small structure at (g-r) $\sim$ -0.5 in the model that is not in the data. This structure is populated by the white dwarfs that are seen in Fig. 4.4.

Another feature can be seen in the model CMD 4.6 along the left most part of the turn off starting at a magnitude of 20. One can see the cyan (halo) stars leave a less densely populated region as the green (thick disk) stars start to slope off to the right. These will be main sequence stars that populate the lowest isochrone, progressing down the isochrone away from the turn off. This can be more evidently seen in Fig. A.2 whereby the stars slope off towards the right where more main sequence stars lie at redder colours. To the left of the turn off resides quite a visible group of stars which are stars that have yet to evolve off the main sequence.

The error in the measurements were plotted and can be see in Fig. A.3 for Pan-STARRS. The error starts to increase after a magnitude of 18 and is greatest around magnitudes of 22. This can explain the spreading out of the Pan-STARRS CMD in Fig. 4.6 where at magnitudes fainter than 18 the spread in colour of the CMD becomes much greater. At these fainter magnitudes the telescopes collect fewer photons per time interval and so the signal to noise ratio decreases, generating higher uncertainties. The same error plot done for 2MASS at the same part of the Kepler field shows an increase in error from magnitudes fainter than 15.

A small investigation was made with regards to the vertical structures seen to see if there was any noticeable change in metallicity. Stars towards the top of the vertical structure from Fig. 4.6 were selected in a magnitude window $12 < m_J < 14$ for 2MASS and $14 < m_g < 16$ for Pan-STARRS, and then had their metallicities plotted against colour. The vertical structures are looked into in terms of colour variance with age later on.

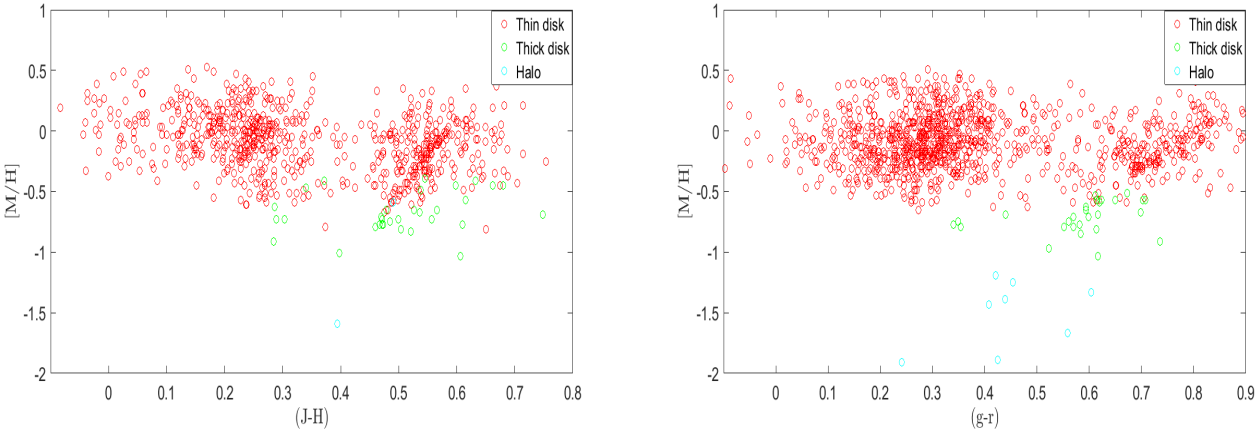

Figure 4.7: Metallicities of vertical towers as a function of colour. There's a similar pattern with the left most structure containing more stars and stars covering a greater range in colour.

4.3 Changing Parameters

When deciding which parameters to investigate and change the obvious choice were related the disks as this comprised almost all of the stars in the total count, the halo contribution being very small. Girardi et al. (2005) states that for high contributions from the young disk one has to look at lower Galactic latitudes which is the case for the Kepler field. The parameters changed were the scale height of the thin disk along with the elimination of extinction, the latter to see mainly what effect it would have on the colour distribution. It was also investigated whether changing the IMF would affect the suitability of the models in both number counts and colour distribution, though for the latter it was expected not to change.

The first parameter that was changed was to set the extinction to zero. With no extinction one would expect the number counts to rise slightly, but the estimate of the increase was difficult to gauge; eliminating extinction would only uncover stars at the limiting magnitude of the passbands. The scale height of the thin disk was increased by increasing α in Equation (3.2) to 2.2 from a default value of 1.66. To be able to observe in clear detail the changes these had on the colour distributions, the stars in a magnitude window were compared. This was decided as $16 < m_g < 18$ for Pan-STARRS and $12 < m_J < 14$ for 2MASS. These ranges give readings with low error whilst still giving sufficient number counts as well as having the two distinct vertical structures.

The distribution functions of the data with the Trilegal runs, including no extinction and a larger thin disk were made. The CDF for the top and bottom of the field for 2MASS are shown in the Fig. 4.8 and 4.9 for Pan-STARRS. What is most noticeable is the difference in closeness of the distributions. The k value from the K-S test increased between each Trilegal run and the observed data from b = 17.6° to b = 6.2°, seen by the

much bigger offset in the figures on the right. In every case the data distribution was redder than its counterparts.

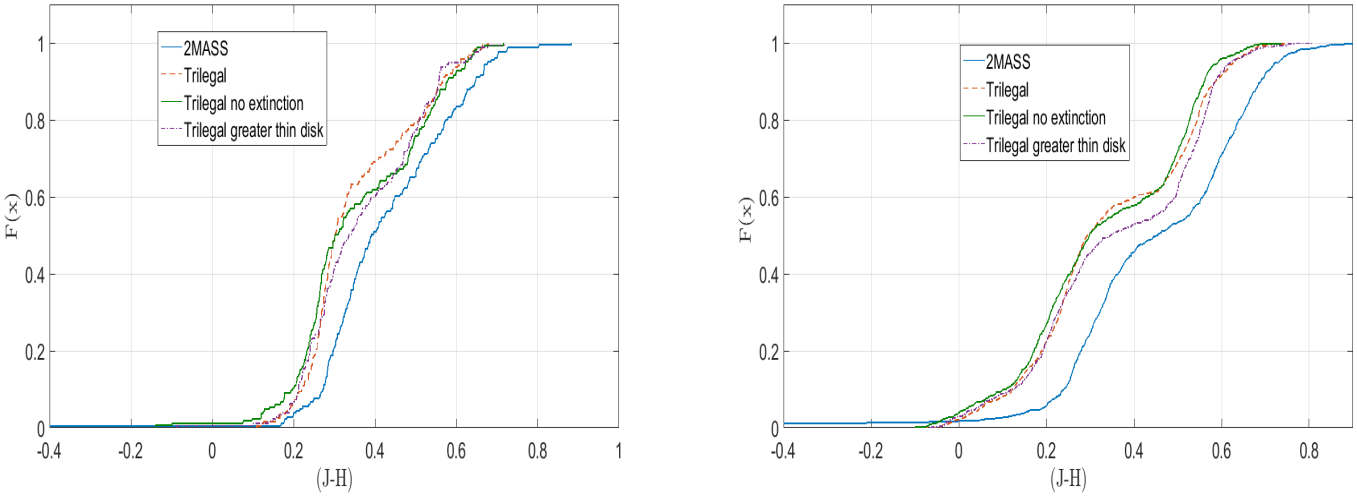

(a) b = 17.6 ° (b) b = 6.2°

Figure 4.8: Cumulative distribution of 2MASS and the different Trilegal runs of stars in $12 < m_J < 14$

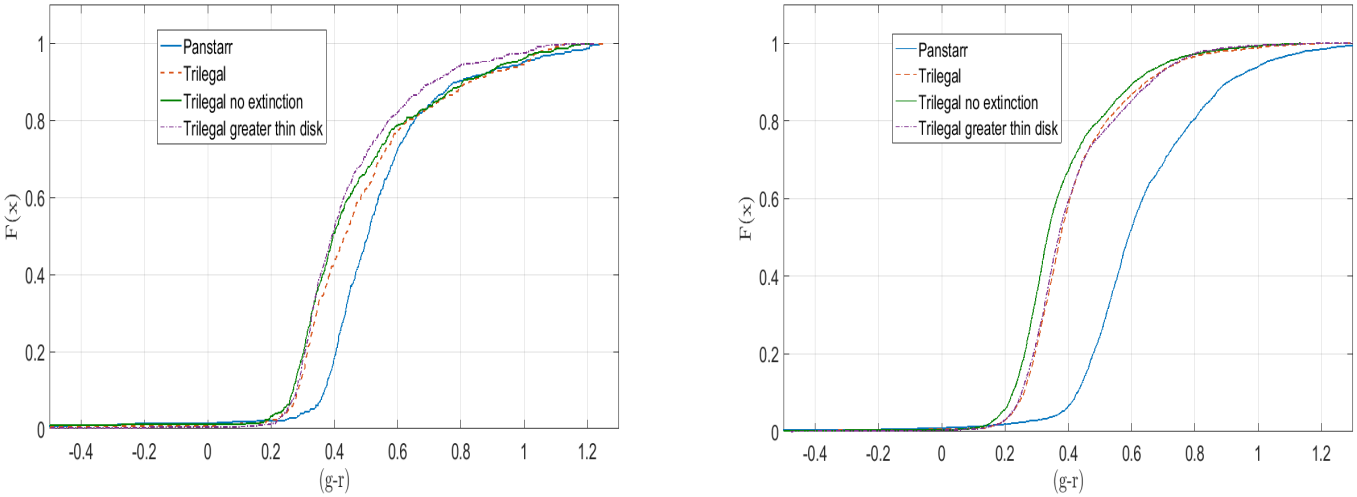

(a) b = 17.6° (b) b = 6.2°

Figure 4.9: Cumulative distribution of Pan-STARRS in the range $16 < m_g < 18$

The distributions for 2MASS look much closer to that of the data for all regions aside from the redder colours of Pan-STARRS at b = 17.6°. Strangely the largest value k statis-

tic from the 2 sided K-S test came from the middle of the Kepler field for 2MASS. More prevalent in the right figure is the lessening of the slopes seen around F(x) = 0.5. This is the transition between the two vertical structures seen in Fig. 4.6.

In every case for both Pan-STARRS and 2MASS the median colour was measured for the data and Trilegal sets.

Table 4.5: Median colour of cumulative distributions

	2MASS			Pan-STARRS		
	b = 6.2°	b = 11°	b = 17.6°	b = 6.2°	b = 11°	b = 17.6°
Data	0.45	0.39	0.37	0.59	0.54	0.51
Trilegal	0.29	0.31	0.30	0.38	0.39	0.43
Trilegal no Extinction	0.29	0.30	0.30	0.33	0.37	0.40
Trilegal greater thin disk	0.35	0.33	0.34	0.37	0.37	0.38

From the top of the Kepler field downwards the median colour became larger, meaning redder distributions for the stars located closer to the bottom of the Kepler field. As one looks closer to the Galactic plane extinction becomes more of an issue, scattering away shorter wavelengths of light more so than longer wavelengths. We see this by the reddening distributions lower in the field for the data distributions. This is not the case for the Trilegal run throughs where in all cases for the three different Trilegal models the opposite was true; the distributions were bluer at the bottom of the Kepler field and became redder towards the top. A two sided K-S test between the data and the different Trilegal catalogues revealed much smaller test statistics for all models at the top of the field.

To supplement the cumulative distributions, histograms of colour were made. The two histograms show that in both cases the Trilegal runs have a bluer turn off, namely around 0.2 each compared to 0.3 for 2MASS and 0.4 for Pan-STARRS. They both show the Trilegal models have slightly bluer distributions.

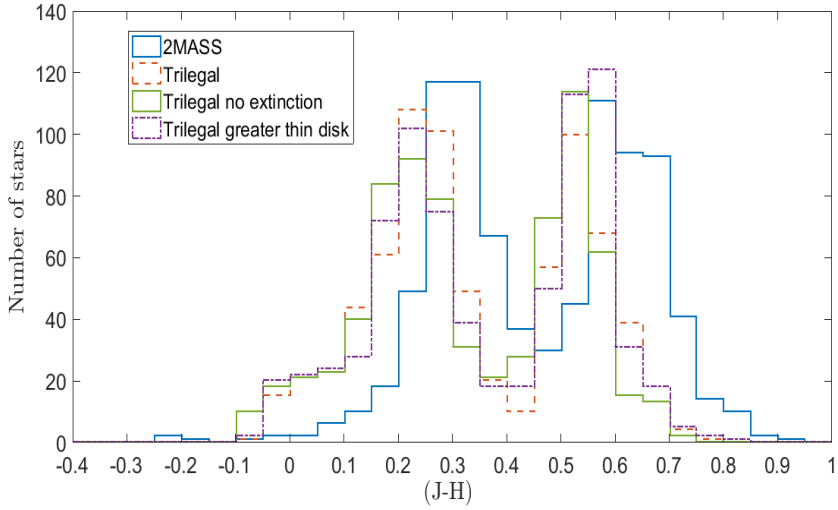

(a) Colour distribution in $12 < m_J < 14$, $b = 6.2°$

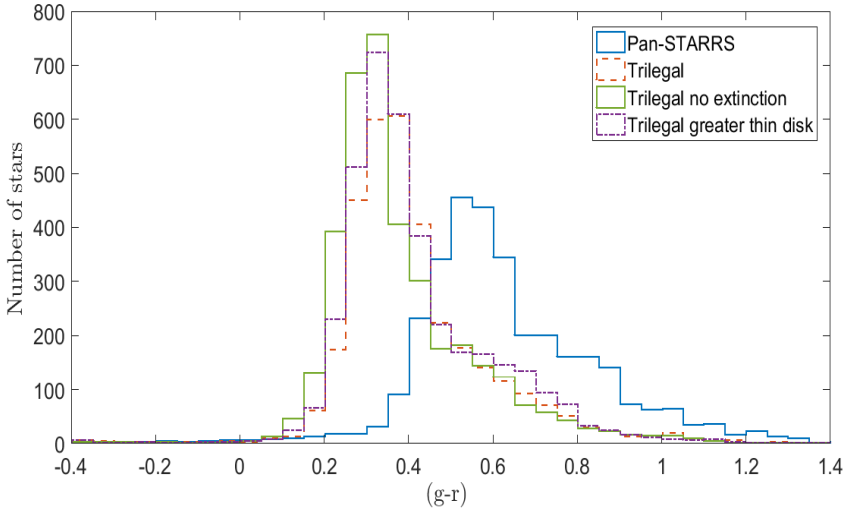

(b) Colour distribution in $16 < m_g < 18$, $b = 6.2°$

Figure 4.10: Colour histograms from Fig. 4.6. The lack of two vertical structures in Pan-STARRS is due to the magnitude range taken which doesn't probe the two vertical structures.

The initial mass function was then investigated to see if there would be a difference in either colour distribution or star counts between the different IMFs. The default Chabrier log normal, Chabrier exponential, Chabrier + Salpeter and Salpeter IMF were pitted against one another. The colour distributions were nearly identical but the star counts varied, significantly in some cases. Using exactly the same parameters as before the different IMFs are shown in Table 4.6

Table 4.6: Number counts in first passband for different IMFs, b = 11°

	Pan-STARRS	2MASS
Data	14 417	3 774
Chabrier lognormal	13 129	3 087
Chabrier exponential	10 737	2 565
Salpeter	4 676	973
Chabrier + Salpeter	10 934	2 580

The Salpeter IMF clearly simulates significantly fewer than the others (64.4 and 68.5% difference from the default IMF) and would be a poor IMF to use for simulating number counts (the distribution was the same as the others). The distributions were tested to see if there would be any change but as expected all were essentially the same. The key differences in IMFs come in the low mass range between 0.05 - 0.2 $M_{\odot}$, and so it would appear that for the IMF to have a significant impact on number counts you have to probe deeper surveys that reach fainter magnitudes. A possible reason for the significant difference in the Salpeter IMF is most likely due to the limiting magnitude chosen for both the models; a limiting magnitude of 17 and 23 doesn't allow for the production of many low mass, faint stars which would have the biggest impact on the Salpeter IMF as it is described solely by a power law giving greater emphasis to stars in the lower mass range.

One final change was made to the input parameters and that was to change the SFR and AMR of the thin disk. The only option is to change to a constant SFR from the default choice. In terms of number counts the changes were negligible, only a 1 008 change in the bottom of the field for Pan-STARRS and 52 for 2MASS. The colour was then plotted as a function of age to see if there was any noticeable change shown in Fig. 4.11. As mentioned earlier the colour of the vertical structures from the CMDs were plotted against the stars age from the same magnitude range as before, $12 < m_J < 14$. Three features of note can be seen. Firstly there is a gap between the stars to the right of the figure and the rest of the stars. The stars to the right are older and these will represent the halo and a small portion of thick disk stars. The stars forming the bulk of the figure to the left are thin disk stars, and the gap in age is 0.12 Gyr. Secondly we note how the bottom structure shows a gradual increase in colour with age. This simply tells us the bluer stars are typically younger. The upper structure does not appear to have the same increase in colour with time, and seems to contain a slightly older population of stars. The last notable feature from the diagram is the few bluest stars seen at far bluer colours than the bottom structure. These represent the blue dwarfs seen earlier and it is clear to see they were born within a similar time frame. Looking back at Fig. 4.7 it can be concluded that the redder vertical structure contains an older population of stars with a slightly lower metal content than the other vertical structure.

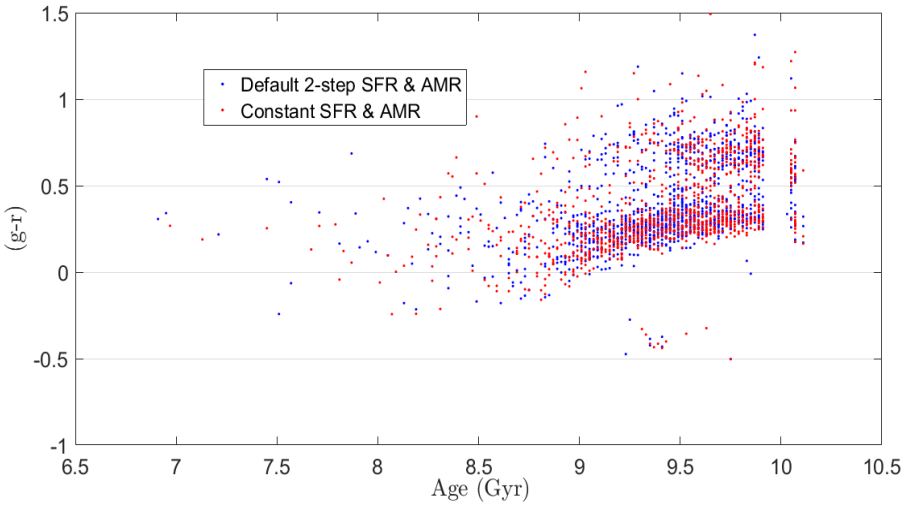

Figure 4.11: Colour plotted against age for Pan-STARRS. These stars are the one seen in $14 < m_g < 16$ from Fig. 4.6. The change in the SFR/AMR gives little change in the distribution of the stars

Chapter 5

Discussion

In this paper the ability of Trilegal to simulate star counts in the two different photometric systems and the colour distributions of these simulated stars are compared to real data in order to see how they vary. The results from this paper sample small star counts and so any conclusions drawn should be tested again on a larger scale to make sure the results are accurate and repeatable. It appears that the accuracy of Trilegal in achieving its goal of simulating expected number counts is comparatively good but depends on Galactic latitude. In every case apart from one Trilegal simulates too few stars as seen in the star count Figures 4.1 and A.1. The same pattern can be seen in Girardi et al. (2005) Fig. 12, where the model appears to simulate slightly too few stars. For 2MASS the percentage change in number counts from the data decreased as you went to higher Galactic latitudes but this is accompanied with greater errors in the number counts per magnitude bin due to the lower counts in general. For Pan-STARRS it is harder to draw the same conclusions since star counts are modelled best in the middle of the Kepler field, and then Trilegal simulates 29% less for the top and 19% more for the bottom of the field.

Making runs with no extinction gave slight changes to number counts, more so for Pan-STARRS. At the top and bottom of the field number counts rose by 3 and 7% respectively whilst for 2MASS there was a 0.8% decrease in number counts for the top and 0.5% increase for the bottom. This follows expectations since extinction, as previously mentioned, is much less of a problem for the infrared survey of 2MASS. The greater change in number counts at low latitudes compared to higher ones for Pan-STARRS shows the effect of the scale height of the extinction disk.

As for the rise in star counts this is best seen through Fig. A.1. From the figures one can see that the fit for 2MASS appears to be much better, especially for fainter magnitudes and that all Trilegal catalogues seem to simulate too many stars at brighter magnitudes. The cumulative distributions, Fig. A.4, show the same trend.

Examining the colour distributions it is evident that Trilegal produces bluer distributions in all cases. This difference in colour is small however and hard to notice from visual comparisons of the CMDs from Fig. 4.6. The comparison of the colour distributions was taken at higher apparent magnitudes so as to reduce the number of readings with high error from the data.

The CDFs of the different Trilegal runs in Fig. 4.9 and Fig. 4.8 reveal that towards the bottom of the Kepler field, Trilegal colour distributions seem to be offset by a larger amount. This is backed up by the results of the K-S test returning greater k values at the bottom of the field. For 2MASS it seems as though Trilegal simulates better results, number counts and colour distributions, the greater the latitude. The same conclusion is difficult to draw about Pan-STARRS, especially due to the number counts but with regards to colour distribution it certainly improves.

This paper has tried to test Trilegal and its ability as a population synthesis code at simulating accurate number counts and photometric data. In doing so stars in the Kepler field were investigated. To be able to say with greater confidence that Trilegal does a good job as a synthesis code one should expand the comparison to other regions of the sky and perhaps different surveys. The Galactic latitudes over which the comparisons in this paper have been made range from only $6 < b < 18$. This is quite a narrow range over which to do the comparisons, however at the same time it allows a greater investigation into the transitions from disk components to halo to be made, albeit there being few halo stars in our study, especially for 2MASS. A change in one magnitude corresponds to a 2.5 times change in the flux, and hence to obtain the same flux one would need to observe the star for 2.5 times longer. Observing fainter magnitudes just might not be practical if the integration time is already large, and so as a result fainter stars, such as those in the halo, are not observed.

Later on in the timetable of the project I realised a problem relating to the size of catalogue table size download, leading to data table sizes smaller than the total data sample. The small sample size of all catalogues was the result of a way to circumnavigate the table size problem. By decreasing the search radius to 0.2 deg^2 allowed for all the results to be downloadable in the table size. Nevertheless, the model predicts star counts with a maximum difference of 29 %. In the paper, Girardi remarks how the model can predict correct number counts with errors smaller than ~ 30 % for all fields located at least 10 degrees above the galactic plane. Our investigation has probed number counts either side of this value and returns a similar result; number counts within 30 % of the correct values.

Had I had more time to work on this project I would have probed these relations but with higher number counts through covering a greater FoV and compared the results to see if there is any significant change for higher counts. A closer look of the extinction parameter was planned to see if changes to this could bring about better results regarding the photometric data as it was clear that the extinction parameter was a shortcoming of the model. Also the model should be tested in more photometric systems; Trilegal offers over 60 photometric systems. The two surveys covered in this paper are not deep surveys and so give only one perspective for the comparison of Trilegal. Perhaps a comparison of a deep survey would be appropriate such as the Deep Multicolour Survey.

5.0.1 Conclusion

In this paper it has been concluded that Trilegal produced bluer distributions compared to that of the surveys. In the paper Sharma et al. (2016), where red giants within the Kepler field are compared to Trilegal, it was found that Trilegal overestimated the number of blue stars. Both these results show a need to refine the model to better represent real photometric data. Models such as Trilegal are needed since they allow the variation of known Parameters which in turn can tell us information about Galactic components. An important reason for the validation of a model such as Trilegal is that in doing so, one can determine where the model may need to be improved. This in turn can lead to improvements in the model and other population synthesis models like it, and help put constraints on Galactic model parameters.

Acknowledgements

I would like to extend my gratitude to Sofia, who's guidance and support through this project has been invaluable and helped keep me on track at times. Her insight and remarks have helped me learn a lot, not just about the project content, but about the research process as a whole and I am very grateful. It has been enjoyable and educational to work under her supervision. Thank you Sofia. I'd also like to thank Lennart for his insightful comments and help in the end of the project.

The Pan-STARRS1 Surveys (PS1) and the PS1 public science archive have been made possible through contributions by the Institute for Astronomy, the University of Hawaii, the Pan-STARRS Project Office, the Max-Planck Society and its participating institutes, the Max Planck Institute for Astronomy, Heidelberg and the Max Planck Institute for Extraterrestrial Physics, Garching, The Johns Hopkins University, Durham University, the University of Edinburgh, the Queen's University Belfast, the Harvard-Smithsonian Center for Astrophysics, the Las Cumbres Observatory Global Telescope Network Incorporated, the National Central University of Taiwan, the Space Telescope Science Institute, the National Aeronautics and Space Administration under Grant No. NNX08AR22G issued through the Planetary Science Division of the NASA Science Mission Directorate, the National Science Foundation Grant No. AST-1238877, the University of Maryland, Eotvos Lorand University (ELTE), the Los Alamos National Laboratory, and the Gordon and Betty Moore Foundation.

This publication makes use of data products from the Two Micron All Sky Survey, which is a joint project of the University of Massachusetts and the Infrared Processing and Analysis Center/California Institute of Technology, funded by the National Aeronautics and Space Administration and the National Science Foundation.

Bibliography

Bensby, T. & Feltzing, S. (2010), The Galactic thin and thick disks in the context of galaxy formation, *in* K. Cunha, M. Spite & B. Barbuy, eds, 'Chemical Abundances in the Universe: Connecting First Stars to Planets', Vol. 265 of *IAU Symposium*, pp. 300–303.

Bland-Hawthorn, J. & Gerhard, O. (2016), 'The Galaxy in Context: Structural, Kinematic, and Integrated Properties', *ARA&A* **54**, 529–596.

Chambers, K. C., Magnier, E. A., Metcalfe, N., Flewelling, H. A., Huber, M. E., Waters, C. Z., Denneau, L., Draper, P. W., Farrow, D., Finkbeiner, D. P., Holmberg, C., Koppenhoefer, J., Price, P. A., Saglia, R. P., Schlafly, E. F., Smartt, S. J., Sweeney, W., Wainscoat, R. J., Burgett, W. S., Grav, T., Heasley, J. N., Hodapp, K. W., Jedicke, R., Kaiser, N., Kudritzki, R.-P., Luppino, G. A., Lupton, R. H., Monet, D. G., Morgan, J. S., Onaka, P. M., Stubbs, C. W., Tonry, J. L., Banados, E., Bell, E. F., Bender, R., Bernard, E. J., Botticella, M. T., Casertano, S., Chastel, S., Chen, W.-P., Chen, X., Cole, S., Deacon, N., Frenk, C., Fitzsimmons, A., Gezari, S., Goessl, C., Goggia, T., Goldman, B., Grebel, E. K., Hambly, N. C., Hasinger, G., Heavens, A. F., Heckman, T. M., Henderson, R., Henning, T., Holman, M., Hopp, U., Ip, W.-H., Isani, S., Keyes, C. D., Koekemoer, A., Kotak, R., Long, K. S., Lucey, J. R., Liu, M., Martin, N. F., McLean, B., Morganson, E., Murphy, D. N. A., Nieto-Santisteban, M. A., Norberg, P., Peacock, J. A., Pier, E. A., Postman, M., Primak, N., Rae, C., Rest, A., Riess, A., Riffeser, A., Rix, H. W., Roser, S., Schilbach, E., Schultz, A. S. B., Scolnic, D., Szalay, A., Seitz, S., Shiao, B., Small, E., Smith, K. W., Soderblom, D., Taylor, A. N., Thakar, A. R., Thiel, J., Thilker, D., Urata, Y., Valenti, J., Walter, F., Watters, S. P., Werner, S., White, R., Wood-Vasey, W. M. & Wyse, R. (2016), 'The Pan-STARRS1 Surveys', *ArXiv e-prints* .

Chomiuk, L. & Povich, M. S. (2011), 'Toward a Unification of Star Formation Rate Determinations in the Milky Way and Other Galaxies', *AJ* **142**, 197.

de Boer, T. J. L., Tolstoy, E., Hill, V., Saha, A., Olsen, K., Starkenburg, E., Lemasle, B., Irwin, M. J. & Battaglia, G. (2012), 'The star formation and chemical evolution history of the sculptor dwarf spheroidal galaxyâ', *A&A* **539**, A103.

Freeman, K. & Bland-Hawthorn, J. (2002), 'The New Galaxy: Signatures of Its Formation', *ARA&A* **40**, 487–537.

Girardi, L., Bertelli, G., Bressan, A., Chiosi, C., Groenewegen, M. A. T., Marigo, P., Salasnich, B. & Weiss, A. (2002), 'Theoretical isochrones in several photometric systems. I. Johnson-Cousins-Glass, HST/WFPC2, HST/NICMOS, Washington, and ESO Imaging Survey filter sets', *A&A* **391**, 195–212.

Girardi, L., Groenewegen, M. A. T., Hatziminaoglou, E. & da Costa, L. (2005), 'Star counts in the Galaxy. Simulating from very deep to very shallow photometric surveys with the TRILEGAL code', *A&A* **436**, 895–915.

Haas, M. R., Batalha, N. M., Bryson, S. T., Caldwell, D. A., Dotson, J. L., Hall, J., Jenkins, J. M., Klaus, T. C., Koch, D. G., Kolodziejczak, J., Middour, C., Smith, M., Sobeck, C. K., Stober, J., Thompson, R. S. & Van Cleve, J. E. (2010), 'Kepler Science Operations', *ApJ* **713**, L115–L119.

Ivezic, Z., Tyson, J. A., Axelrod, T., Burke, D., Claver, C. F., Cook, K. H., Kahn, S. M., Lupton, R. H., Monet, D. G., Pinto, P. A., Strauss, M. A., Stubbs, C. W., Jones, L., Saha, A., Scranton, R., Smith, C. & LSST Collaboration (2009), LSST: From Science Drivers To Reference Design And Anticipated Data Products, *in* 'American Astronomical Society Meeting Abstracts #213', Vol. 41 of *Bulletin of the American Astronomical Society*, p. 366.

Komatsu, E., Smith, K. M., Dunkley, J., Bennett, C. L., Gold, B., Hinshaw, G., Jarosik, N., Larson, D., Nolta, M. R., Page, L., Spergel, D. N., Halpern, M., Hill, R. S., Kogut, A., Limon, M., Meyer, S. S., Odegard, N., Tucker, G. S., Weiland, J. L., Wollack, E. & Wright, E. L. (2011), 'Seven-year Wilkinson Microwave Anisotropy Probe (WMAP) Observations: Cosmological Interpretation', *ApJ* **192**, 18.

Minniti, D. & Zoccali, M. (2008), The Galactic bulge: a review, *in* M. Bureau, E. Athanassoula & B. Barbuy, eds, 'Formation and Evolution of Galaxy Bulges', Vol. 245 of *IAU Symposium*, pp. 323–332.

Sharma, S., Stello, D., Bland-Hawthorn, J., Huber, D. & Bedding, T. R. (2016), 'Stellar Population Synthesis Based Modeling of the Milky Way Using Asteroseismology of 13,000 Kepler Red Giants', *ApJ* **822**, 15.

Skrutskie, M. F., Cutri, R. M., Stiening, R., Weinberg, M. D., Schneider, S., Carpenter, J. M., Beichman, C., Capps, R., Chester, T., Elias, J., Huchra, J., Liebert, J., Lonsdale, C., Monet, D. G., Price, S., Seitzer, P., Jarrett, T., Kirkpatrick, J. D., Gizis, J. E., Howard, E., Evans, T., Fowler, J., Fullmer, L., Hurt, R., Light, R., Kopan, E. L., Marsh, K. A., McCallon, H. L., Tam, R., Van Dyk, S. & Wheelock, S. (2006), 'The Two Micron All Sky Survey (2MASS)', *AJ* **131**, 1163–1183.

Snaith, O., Haywood, M., Di Matteo, P., Lehnert, M. D., Combes, F., Katz, D. & Gómez, A. (2015), 'Reconstructing the star formation history of the Milky Way disc(s) from chemical abundances', *A&A* **578**, A87.

Tonry, J. L., Stubbs, C. W., Lykke, K. R., Doherty, P., Shivvers, I. S., Burgett, W. S., Chambers, K. C., Hodapp, K. W., Kaiser, N., Kudritzki, R.-P., Magnier, E. A., Morgan, J. S., Price, P. A. & Wainscoat, R. J. (2012), 'The Pan-STARRS1 Photometric System', *ApJ* **750**, 99.

Vanhollebeke, E., Groenewegen, M. A. T. & Girardi, L. (2009), 'Stellar populations in the Galactic bulge. Modelling the Galactic bulge with TRILEGAL', *A&A* **498**, 95–107.

Appendix A

Additional figures

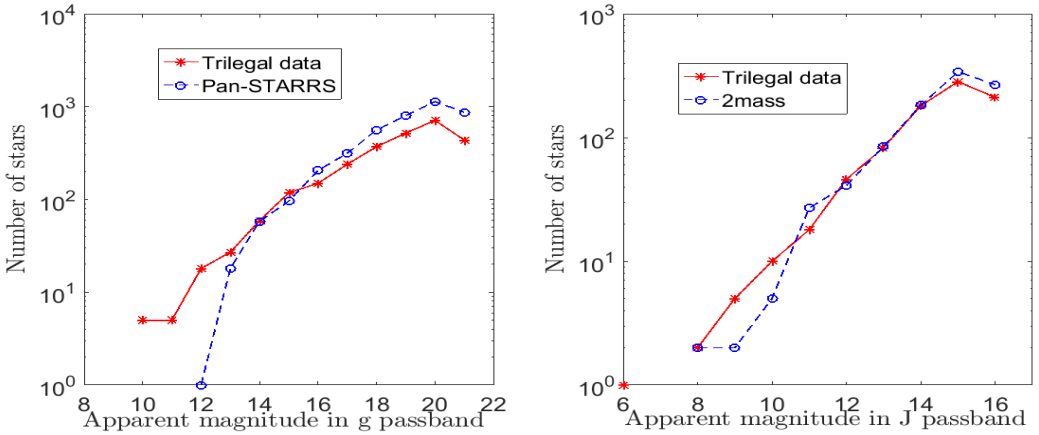

(a) b = 17.6°

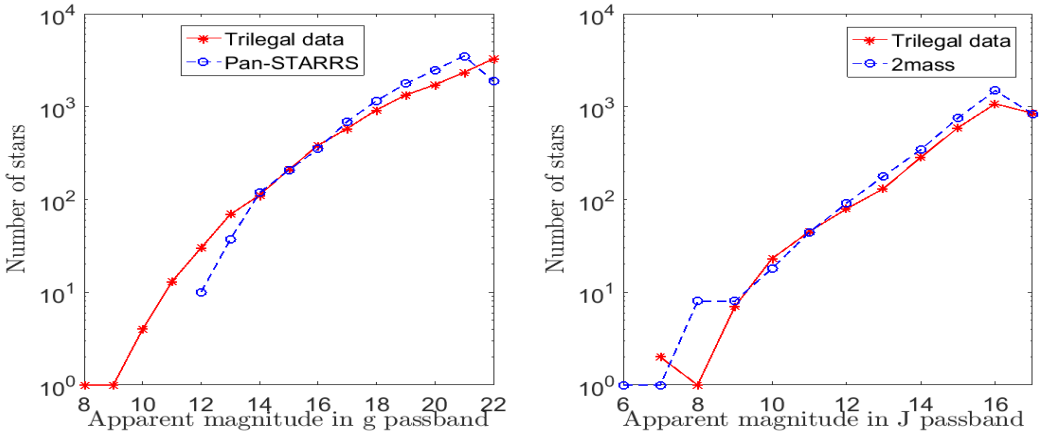

(b) b = 11°

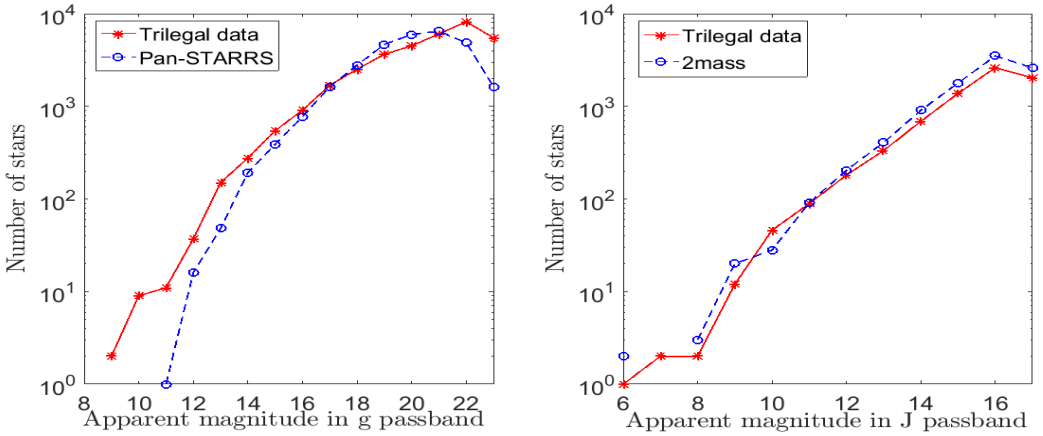

(c) b = 6.2°

Figure A.1: Star count for Panstarrs and 2MASS in the different search catalogues within the Kepler field. The aforementioned completeness limit was taken into account, and as such the magnitude cut off points were chosen when the Number count started to decrease.

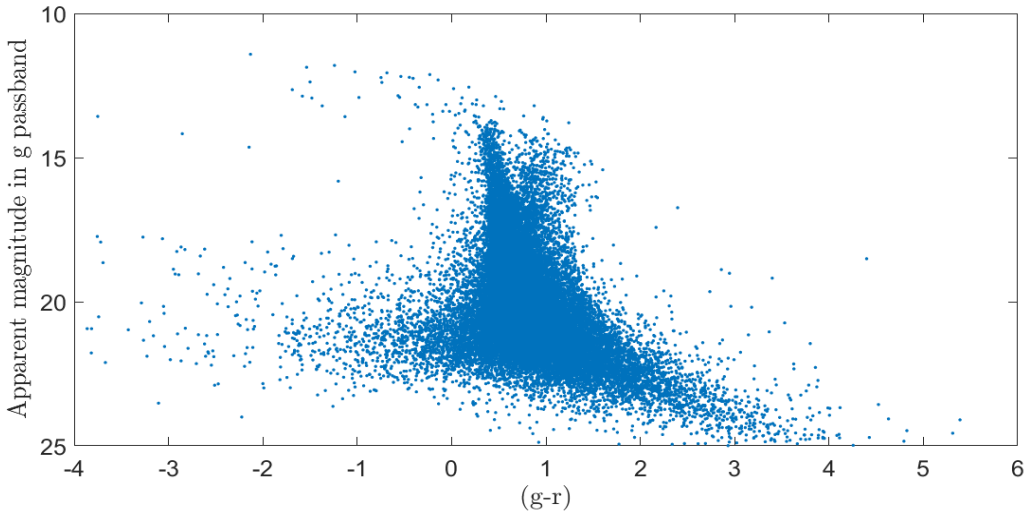

Figure A.2: Zoomed out Pan-STARRS CMD from Fig. 4.6

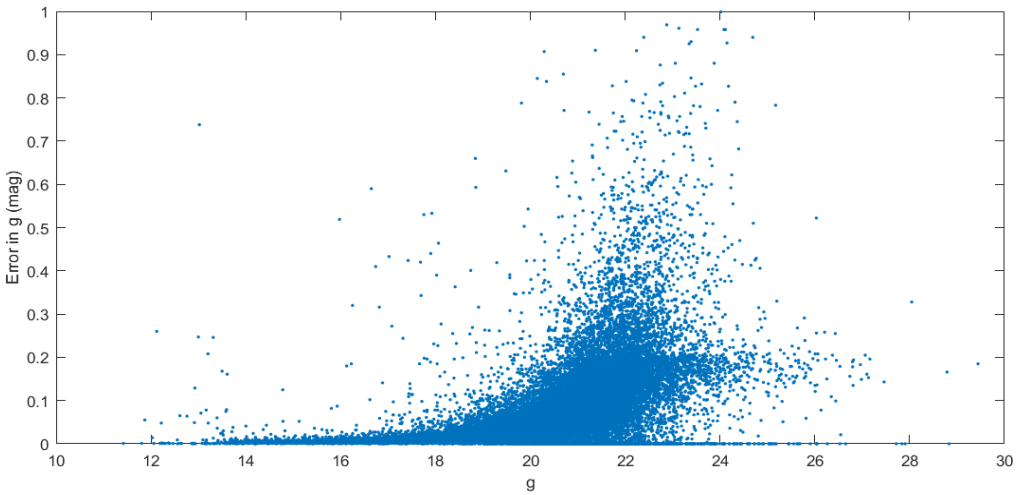

Figure A.3: Error in Pan-STARR g band readings for bottom of Kepler field.

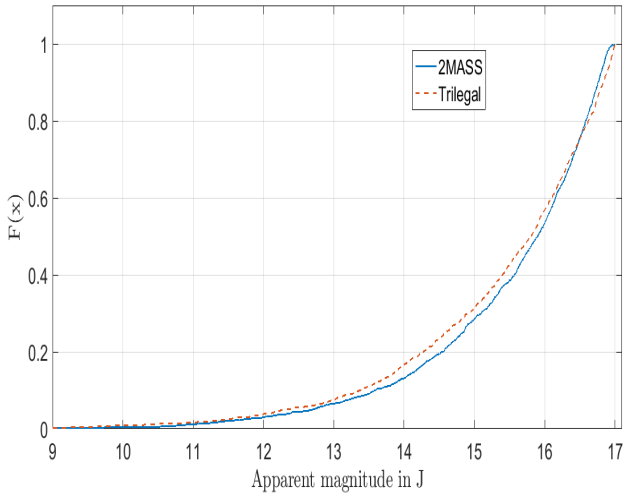

(a) b = 17.6°

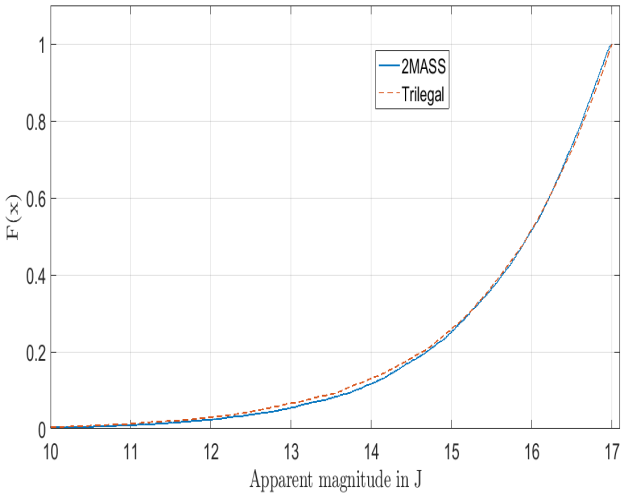

(b) b = 6.2°

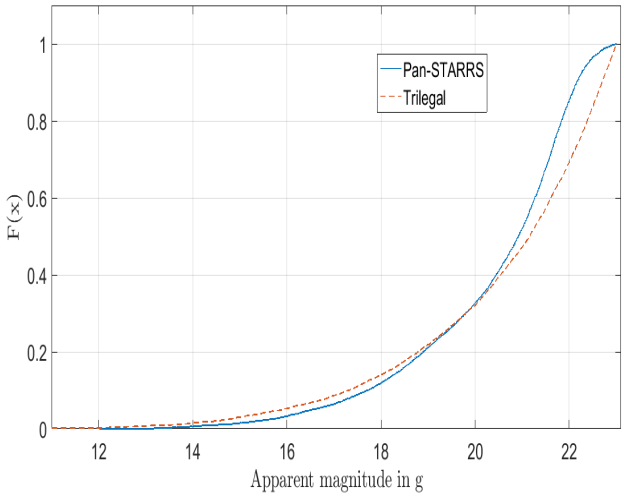

(c) b = 17.6°

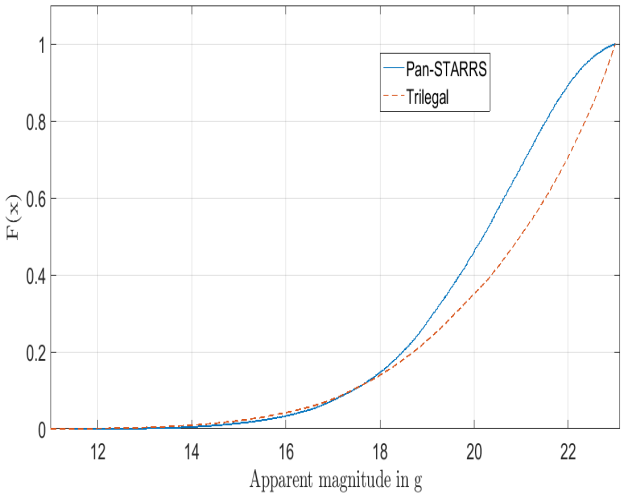

(d) b = 6.2°

Figure A.4: Cumulative distribution of 2MASS J and Pan-STARRS g band with the cut off at $m_J = 17$ and $m_g = 23$